



ELSEVIER

Journal of Power Sources 93 (2001) 141–144

JOURNAL OF  
POWER  
SOURCES

www.elsevier.com/locate/jpowersour

# Activation behavior of the Zr-based Laves phase alloy electrode

Cao Jiansheng<sup>a,\*</sup>, Gao Xueping<sup>a</sup>, Lin Dongfeng<sup>a</sup>, Zhou Xingdi<sup>b</sup>,  
Yuan Huatang<sup>a</sup>, Song Deying<sup>a</sup>, Shen Panwen<sup>a</sup>

<sup>a</sup>Institute of New Energy Material Chemistry, Nankai University, Weijin Road 94#, Tianjin 300071, China

<sup>b</sup>Department of Chemistry, Nankai University, Weijin Road 94#, Tianjin 300071, China

Received 22 October 1999; received in revised form 4 July 2000; accepted 8 August 2000

## Abstract

The poor activation of the Zr-based AB<sub>2</sub> Laves phase alloy hydride electrode is one of the problems retarding their commercialization. A surface treatment technique was carried out here to improve the poor activation of the alloys Zr(V<sub>0.1</sub>Mn<sub>0.3</sub>Ni<sub>0.6</sub>)<sub>2</sub>, Zr(V<sub>0.1</sub>Mn<sub>0.3</sub>Ni<sub>0.6</sub>Co<sub>0.05</sub>)<sub>2</sub>, ZrTi<sub>0.1</sub>(V<sub>0.1</sub>Mn<sub>0.3</sub>Ni<sub>0.6</sub>Co<sub>0.05</sub>)<sub>2</sub> and ZrTi<sub>0.1</sub>(V<sub>0.1</sub>Mn<sub>0.3</sub>Ni<sub>0.6</sub>Co<sub>0.05</sub>Cr<sub>0.05</sub>)<sub>2</sub>. We pre-treated the alloy powders by immersing and stirring them in solution of NH<sub>4</sub>F/NiCl<sub>2</sub> to make the alloy surface clean and form a layer of nickel-rich, which has been regarded as an indispensable factor for the electrochemical activity of the alloy. It was found that the activation of the alloy electrode has been greatly improved by this method. The discharge capacity of the electrodes made from the treated alloy powder is over 345 mA h g<sup>-1</sup> at the discharge current density of 100 mA g<sup>-1</sup>. Especially, the alloy electrode of the treated ZrTi<sub>0.1</sub>(V<sub>0.1</sub>Mn<sub>0.3</sub>Ni<sub>0.6</sub>Co<sub>0.05</sub>Cr<sub>0.05</sub>)<sub>2</sub> gives a discharge capacity of 390 mA h g<sup>-1</sup> at the first cycle, however, the discharge capacity of the untreated alloy electrode is only 42 mA h g<sup>-1</sup> at the first cycle. The analysis of X-ray diffraction (XRD) shows that the alloy of crystal structure is a cubic AB<sub>2</sub> Laves phase. The different activation property of the alloy electrode was analyzed on the basis of surface examination by scanning electron microscope (SEM), specific surface area (SSA) and X-ray photoelectron spectroscopy (XPS). © 2001 Elsevier Science B.V. All rights reserved.

**Keywords:** Laves phase alloy; Activation; Surface treatment; Nickel-rich layer

## 1. Introduction

As an excellent negative electrode material in nickel-metal hydride battery, hydrogen storage alloys attracting considerable attention all over the world have been investigated intensively and commercialized to meet the social needs because they have high energy density and are friendly to the environment and so on [1–3]. At present, the most widely developed and commercialized electrode materials in such battery belong to the AB<sub>5</sub>-type hydrogen storage alloy. However, another kind of hydrogen storage alloys, AB<sub>2</sub>-type (A = Zr, Ti; B = Ni, Mn, Cr, etc.). Laves phase alloys possessing larger hydrogen storage capacity than the AB<sub>5</sub>-type alloy, have been regarded as a new generation of hydrogen storage alloy. Generally speaking, the main problems hindering the practical application of Laves phase alloys are slow activation and low high-rate capability because of a formation of the oxide layer on the alloy surface. Among them, the slow activation is a very important factor that should be solved at first. In general, the reason of poor activation is that a thin but dense and passive

oxide layer exists on the alloy surface and it decreases the electrocatalytic activity for hydrogen absorption–desorption (charging–discharging).

In order to overcome the shortcoming, some modifications have been carried out recent years. Gao et al. [4] have reported that the F-treated Zr(V<sub>0.2</sub>Mn<sub>0.2</sub>Ni<sub>0.6-x</sub>Co<sub>x</sub>)<sub>2.4</sub> electrode showed excellent activation and a high initial discharge capacity owing to the increase of specific surface area (SSA) and the formation of nickel-rich surface layer in the F-treated alloy. Choi et al. [5] investigated the properties of Zr<sub>0.9</sub>Ti<sub>0.1</sub>Ni<sub>1.1</sub>Co<sub>0.1</sub>Mn<sub>0.6</sub>V<sub>0.2</sub> by immersing the electrode in a boiling KOH solution. They found that a thicker Ni layer was identified on the pre-treated alloy electrode as a catalyst and determines the electrode performance. Sun et al. [6] used the mechanical ball-milling to coat nickel particles on the surface of Zr(Cr<sub>0.4</sub>Ni<sub>0.6</sub>)<sub>2</sub> and they found the activation process for the electrode was apparently shorted after coating Ni on the alloy. McCormack et al. [7] have reported the activation of ZrCrNi was greatly accelerated by a pulse activation process consisting of altering applying potential pulses at voltages expected to result in hydriding–dehydriding of the electrode because of the formation of microcracks. Iwakura et al. [8] improved the activation of ZrV<sub>0.5</sub>Mn<sub>0.5</sub>Ni

\* Corresponding author. Fax: +86-22-2350-2604.

alloy electrodes by immersing the electrode in an alkaline solution containing  $\text{KBH}_4$  as a reducing agent. They observed absorption of hydrogen atom released from  $\text{BH}_4^-$ , which produce a new surface of the alloy owing to expansion. Jung et al. [9] studied the activation of  $\text{Zr}_{0.7}\text{Ti}_{0.3}\text{Cr}_{0.3}\text{Mn}_{0.3}\text{V}_{0.4}\text{Ni}$  by immersing electrodes in hot alkaline and charging simultaneously, resulting in the formation of cracks and a new clean surface. Furthermore, they observed that Ni with high catalytic activity was enriched on the alloy surface. Sun et al. [10] added a small quantity of lanthanum or cerium in  $\text{ZrNi}_{1.2}\text{Mn}_{0.6}\text{V}_{0.2}\text{Cr}_{0.1}$  to improve the activation behaviors. It is found that La or Ce does not dissolve in the cubic C15 Laves phase, but combines preferentially with nickel to form  $\text{LaNi}$  or  $\text{CeNi}$  that act as ‘active sites’, where hydrogen atoms penetrate through the oxide layer and form  $\text{LaNiH}_x$  or  $\text{CeNiH}_x$  hydride. Wang et al. [11] observed that the activity properties of  $\text{ZrTiV}$  alloy electrode were improved by an oxidation treatment that resulted in the segregation of zirconium and titanium on the alloy surface, while metallic nickel and vanadium precipitated in the subsurface.

Generally, most activation process is accompanied with the appearance of both a new and clean surface and a layer of nickel-rich on the surface or subsurface of the hydrogen storage alloy. So, an effective modified surface treatment technique was adopted to make the alloy surface clean and enrich metallic Ni on the alloy surface. In order to get a thicker layer of nickel-rich that has good catalytic effect on electrochemical reaction,  $\text{NiCl}_2$  was added into the  $\text{NH}_4\text{F}$  solution to improve the activation property well. Four kinds of Laves phase alloy  $\text{Zr}(\text{V}_{0.1}\text{Mn}_{0.3}\text{Ni}_{0.6})_2$ ,  $\text{Zr}(\text{V}_{0.1}\text{Mn}_{0.3}\text{Ni}_{0.6}\text{Co}_{0.05})_2$ ,  $\text{ZrTi}_{0.1}(\text{V}_{0.1}\text{Mn}_{0.3}\text{Ni}_{0.6}\text{Co}_{0.05})_2$  and  $\text{ZrTi}_{0.1}(\text{V}_{0.1}\text{Mn}_{0.3}\text{Ni}_{0.6}\text{Co}_{0.05}\text{Cr}_{0.05})_2$  were chosen and treated by this way to shorten their activation number.

## 2. Experimental

The Laves phase alloy samples in this investigation, namely,  $\text{Zr}(\text{V}_{0.1}\text{Mn}_{0.3}\text{Ni}_{0.6})_2$ ,  $\text{Zr}(\text{V}_{0.1}\text{Mn}_{0.3}\text{Ni}_{0.6}\text{Co}_{0.05})_2$ ,  $\text{ZrTi}_{0.1}(\text{V}_{0.1}\text{Mn}_{0.3}\text{Ni}_{0.6}\text{Co}_{0.05})_2$  and  $\text{ZrTi}_{0.1}(\text{V}_{0.1}\text{Mn}_{0.3}\text{Ni}_{0.6}\text{Co}_{0.05}\text{Cr}_{0.05})_2$ , were synthesized by arc-melting technique in an argon atmosphere from the starting elements (3 N purity). Each ingot was turned over and remelted four times to ensure the homogeneity of the alloys. Then, the alloys were annealed in an argon atmosphere at  $1050^\circ\text{C}$  for 7 h. In 100 ml solution containing  $\text{NH}_4\text{F}$  ( $0.216 \text{ mol l}^{-1}$ ) and  $\text{NiCl}_2$  ( $0.0168 \text{ mol l}^{-1}$ ), 4 g alloy powder was treated at  $70^\circ\text{C}$  for 30 min after the alloy was pulverized.

Crystal structure was characterized by Rigakudmax X-ray diffraction (XRD) using  $\text{Cu K}\alpha$  radiation. The SSA was measured by the method of BET (Braunauer–Emmett–Teller). The elements in a  $\text{NH}_4\text{F}/\text{NiCl}_2$  solution both before and after treatment were analyzed by the means of inductively coupled plasma spectroscopy (ICPS). Surface morphology of the alloy samples before and after treatment was

analyzed by scanning electron microscopy (SEM). The surface chemical state and composition of the sample were measured by means of X-ray photoelectron spectroscopy (XPS).

The alloy electrodes were prepared by cold pressing the mixture of different sample and nickel powder in the weight of 1:3 to form a pellet of 10 mm in diameter and 1.4 mm in thickness under a mechanic load of 3 MPa. The electrode was tested in a standard open trielectrode electrolysis cell, in which an alloy electrode acted as a working electrode, a  $\text{Hg}/\text{HgO}$  (in 6 N KOH) electrode acted as a reference electrode, a  $\text{Ni}(\text{OH})_2/\text{NiOOH}$  electrode acted as a counter electrode. The discharge capacity of the alloy electrodes was measured using a galvanostatic charge–discharge apparatus. The electrode was charged with a current density of  $100 \text{ mA g}^{-1}$  for 5 h and discharged with the same current density to the cut-off potential set at  $-0.6 \text{ V}$ .

## 3. Results and discussions

Fig. 1 shows that the XRD patterns of the treated alloy powders are identical with those of untreated. From the results obtained, it can be seen that the alloys  $\text{Zr}(\text{V}_{0.1}\text{Mn}_{0.3}\text{Ni}_{0.6}\text{Co}_{0.05})_2$ ,  $\text{Zr}(\text{Ti}_{0.1}\text{V}_{0.1}\text{Mn}_{0.3}\text{Ni}_{0.6}\text{Co}_{0.05})_2$  and  $\text{ZrTi}_{0.1}(\text{V}_{0.1}\text{Mn}_{0.3}\text{Ni}_{0.6}\text{Co}_{0.05}\text{Cr}_{0.05})_2$  were identified to be single phase and have a C15 cubic Laves phase structure. On the other hand, the alloy  $\text{Zr}(\text{V}_{0.1}\text{Mn}_{0.3}\text{Ni}_{0.6})_2$  shows a multiphase structure. The main phase of it also exhibits a C15 cubic Laves phase structure and the extra peak on  $2\theta = 37.8^\circ$  belongs to orthorhombic  $\text{Zr}_7\text{Ni}_{10}$ .

Fig. 2 shows the discharge capacity of the eight kinds of electrodes versus discharge cycle. It can be seen that the discharge capacity of the untreated alloy electrodes slowly increases with cycling. The untreated alloy  $\text{ZrTi}_{0.1}(\text{V}_{0.1}\text{Mn}_{0.3}\text{Ni}_{0.6}\text{Co}_{0.05}\text{Cr}_{0.05})_2$  shows the poorest activation property, which only offers a capacity of  $42 \text{ mA h g}^{-1}$  at the first cycle. However, the treated alloy electrodes showed an excellent kinetics without activation process and reached the large discharge capacity at the first cycle. In particular, the treated alloy  $\text{ZrTi}_{0.1}(\text{V}_{0.1}\text{Mn}_{0.3}\text{Ni}_{0.6}\text{Co}_{0.05}\text{Cr}_{0.05})_2$  shows the best activation property giving discharge capacity of  $390 \text{ mA h g}^{-1}$  at the first cycle.

Table 1 shows the concentration of the elements in the  $\text{NH}_4\text{F}/\text{NiCl}_2$  solution measured by ICPS both before and after treating the alloy  $\text{Zr}(\text{V}_{0.1}\text{Mn}_{0.3}\text{Ni}_{0.6}\text{Co}_{0.05})_2$ . It can be seen that the elements of the alloy have been dissolved into the  $\text{NH}_4\text{F}/\text{NiCl}_2$  solution partly, the relative concentration of

Table 1  
The concentration of the elements in the  $\text{NH}_4\text{F}/\text{NiCl}_2$  solution before and after treating the alloy  $\text{Zr}(\text{V}_{0.1}\text{Mn}_{0.3}\text{Ni}_{0.6}\text{Co}_{0.05})_2$  ( $\mu\text{g ml}^{-1}$ )

Solution	Ni	Zr	V	Mn	Co
Before treatment	931.85				
After treatment	17.84	847.25	38.12	314.00	11.26

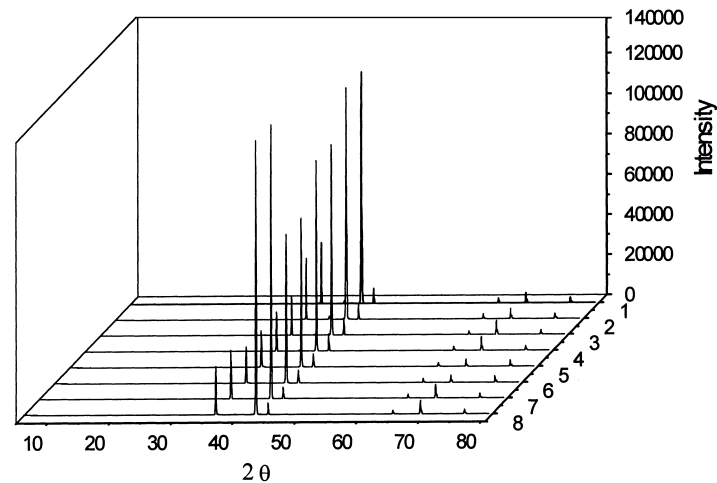


Fig. 1. The X-ray diffraction patterns of the alloy powders. (1, 3, 5, 7: untreated alloy; 2, 4, 6, 8: treated alloy) 1, 2:  $\text{Zr}(\text{V}_{0.1}\text{Mn}_{0.3}\text{Ni}_{0.6})_2$ ; 3, 4:  $\text{Zr}(\text{V}_{0.1}\text{Mn}_{0.3}\text{Ni}_{0.6}\text{Co}_{0.05})_2$ ; 5, 6:  $\text{ZrTi}_{0.1}(\text{V}_{0.1}\text{Mn}_{0.3}\text{Ni}_{0.6}\text{Co}_{0.05})_2$ ; 7, 8:  $\text{ZrTi}_{0.1}(\text{V}_{0.1}\text{Mn}_{0.3}\text{Ni}_{0.6}\text{Co}_{0.05}\text{Cr}_{0.05})_2$ .

dissolved Zr, Mn, Co and V is 847.25, 314.00, 11.26 and  $38.12 \mu\text{g ml}^{-1}$ , respectively. It is interesting to find that the concentration of  $\text{Ni}^{2+}$  ion decreases drastically from  $931.85 \mu\text{g ml}^{-1}$  before treatment to  $17.84 \mu\text{g ml}^{-1}$  after treatment. This phenomenon indicated that the Ni metal has been enriched on the surface of the alloy powder. The basic mechanism of Ni deposition was discussed here. The alloy surface formed an oxide layer of all the metal elements after pulverized [12]. And it became a surface of metal elements after  $\text{NH}_4\text{F}$  reacted on all kinds of oxides. Then, all the metal elements on the alloy (except Ni) displaced the  $\text{Ni}^{2+}$  in  $\text{NiCl}_2$  because that the potential of  $\text{Ni}^{2+}/\text{Ni}$  is higher than the potentials of others such as  $\text{Zr}^{4+}/\text{Zr}$ ,  $\text{Mn}^{2+}/\text{Mn}$ , etc. [13]. So, Ni was deposited on the alloy surface.

Fig. 3 shows the SEM photographs of the treated and untreated alloy powder of  $\text{ZrTi}_{0.1}(\text{V}_{0.1}\text{Mn}_{0.3}\text{Ni}_{0.6}$

$\text{Co}_{0.05}\text{Cr}_{0.05})_2$ . It has been observed that the surface of the treated alloy powders became rougher very much than the untreated and there are many microcracks on the surface of the alloy powder. This kind of morphology implied that a fresh and clean surface formed when using surface treatment. It is important to point out that the surface is a nickel-rich layer having a high catalytic activity, which was deduced from the following XPS data. It can be assumed naturally that the SSA of the alloy powder must have become larger than the untreated one.  $\text{ZrTi}_{0.1}(\text{V}_{0.1}\text{Mn}_{0.3}\text{Ni}_{0.6}\text{Co}_{0.05}\text{Cr}_{0.05})_2$  was chosen as an example to evaluate the SSA of the untreated alloy powder by the method of BET and its SSA was  $0.25 \text{ m}^2 \text{ g}^{-1}$ . Nevertheless, the SSA of the powders of the treated alloys  $\text{Zr}(\text{V}_{0.1}\text{Mn}_{0.3}\text{Ni}_{0.6})_2$ ,  $\text{Zr}(\text{V}_{0.1}\text{Mn}_{0.3}\text{Ni}_{0.6}\text{Co}_{0.05})_2$ ,  $\text{ZrTi}_{0.1}(\text{V}_{0.1}\text{Mn}_{0.3}\text{Ni}_{0.6}\text{Co}_{0.05})_2$  and  $\text{ZrTi}_{0.1}(\text{V}_{0.1}\text{Mn}_{0.3}\text{Ni}_{0.6}\text{Co}_{0.05}\text{Cr}_{0.05})_2$  is 0.34, 0.41, 0.63 and  $0.60 \text{ m}^2 \text{ g}^{-1}$ , respectively. The SSA of the powder

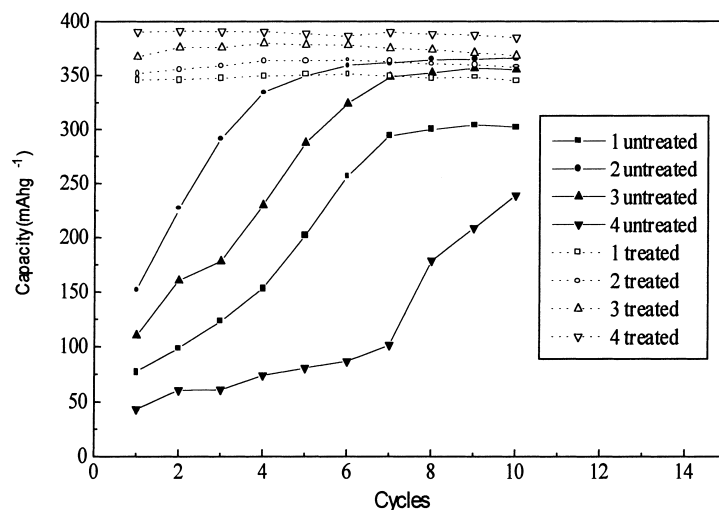


Fig. 2. The discharge capacity of the eight kinds of electrodes versus discharge cycles. 1:  $\text{Zr}(\text{V}_{0.1}\text{Mn}_{0.3}\text{Ni}_{0.6})_2$ ; 2:  $\text{Zr}(\text{V}_{0.1}\text{Mn}_{0.3}\text{Ni}_{0.6}\text{Co}_{0.05})_2$ ; 3:  $\text{ZrTi}_{0.1}(\text{V}_{0.1}\text{Mn}_{0.3}\text{Ni}_{0.6}\text{Co}_{0.05})_2$ ; 4:  $\text{ZrTi}_{0.1}(\text{V}_{0.1}\text{Mn}_{0.3}\text{Ni}_{0.6}\text{Co}_{0.05}\text{Cr}_{0.05})_2$ .

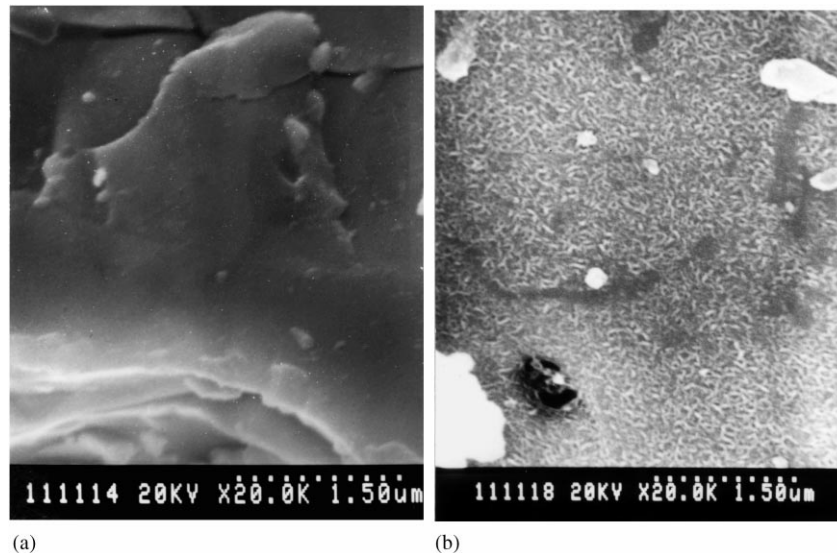


Fig. 3. The SEM photographs of the untreated (a) and treated (b) alloy powder of  $\text{ZrTi}_{0.1}(\text{V}_{0.1}\text{Mn}_{0.3}\text{Ni}_{0.6}\text{Co}_{0.05}\text{Cr}_{0.05})_2$ .

Table 2

The relative atomic concentration on the surface of the alloy  $\text{ZrTi}_{0.1}(\text{V}_{0.1}\text{Mn}_{0.3}\text{Ni}_{0.6}\text{Co}_{0.05}\text{Cr}_{0.05})_2$  (%)

Alloy	Ni	Zr	Ti	V	Mn	Cr	Co
Untreated powder	1.72	68.04	5.53	5.64	12.12	4.31	2.59
Treated powder	31.0	16.43	9.11	22.46	5.85	8.44	6.76

of the treated alloy  $\text{ZrTi}_{0.1}(\text{V}_{0.1}\text{Mn}_{0.3}\text{Ni}_{0.6}\text{Co}_{0.05}\text{Cr}_{0.05})_2$  is 2.4 times larger than that of the untreated.

XPS analysis was carried out in order to investigate the effect of the surface treatment on the surface of the alloy. Table 2 shows the relative atomic concentration on the surface of the alloy  $\text{ZrTi}_{0.1}(\text{V}_{0.1}\text{Mn}_{0.3}\text{Ni}_{0.6}\text{Co}_{0.05}\text{Cr}_{0.05})_2$ . It was found that Zr decreased from 68.04 to 16.45%, but Ni increases from 1.72 to 31.00%. This result means the dense Zr oxide layer is broken and a nickel-rich layer is formed. It is believed that abundant Ni on the alloy surface activates the alloy easily. And the result obtained here is of agreement with that of ICPS we have discussed in the former section.

#### 4. Conclusions

The poor activation property of the hydride electrodes made of Zr-based  $\text{AB}_2$  Laves phase alloys  $\text{Zr}(\text{V}_{0.1}\text{Mn}_{0.3}\text{Ni}_{0.6})_2$ ,  $\text{Zr}(\text{V}_{0.1}\text{Mn}_{0.3}\text{Ni}_{0.6}\text{Co}_{0.05})_2$ ,  $\text{ZrTi}_{0.1}(\text{V}_{0.1}\text{Mn}_{0.3}\text{Ni}_{0.6}\text{Co}_{0.05})_2$  and  $\text{ZrTi}_{0.1}(\text{V}_{0.1}\text{Mn}_{0.3}\text{Ni}_{0.6}\text{Co}_{0.05}\text{Cr}_{0.05})_2$  has been greatly improved by the method of immersing and stirring the alloy powder in  $\text{NH}_4\text{F}/\text{NiCl}_2$  solution. The result obtained was attributed to the formation of a new and clean surface and a nickel-rich layer on the treated alloy observed by the analysis of XRD, SEM, SSA and XPS on the both treated

and untreated alloys. This kind of surface treatment might be used for the other hydrogen storage alloys that have slow activation property to shorten their hydriding–dehydriding (charge–discharge) cycling for activation.

#### Acknowledgements

The authors are grateful for the financial support of the Doctor Foundation from the Ministry of Education of China, and Natural Science Foundation from Tianjin of China.

#### References

- [1] Y. Liu, X. Zhang, *J. Alloys Comp.* 267 (1998) 231.
- [2] H.S. Lim, G.R. Zelter, D.U. Allison, R.E. Haun, *J. Power Source* 66 (1997) 101.
- [3] T. Vogt, J.J. Reilly, J.R. Johnson, G.D. Adzic, J. McBreen, *J. Electrochem. Soc.* 146 (1) (1999) 15.
- [4] X.P. Gao, S.H. Ye, J. Liu, D.Y. Song, Y.S. Zhang, *Int. J. Hydrogen Energy* 23 (1998) 781.
- [5] W.-K. Choi, K. Yamataka, S.G. Zhang, H. Inoue, C. Iwakura, *J. Electrochem. Soc.* 146 (1) (1999) 46.
- [6] D. Sun, M. Latroche, A. Percheron-Guégan, *J. Alloys Comp.* 257 (1997) 302.
- [7] M. McCormack, M.E. Badding, B. Vyas, S.M. Zahurak, D.W. Murphy, *J. Electrochem. Soc.* 143 (1996) L31.
- [8] C. Iwakura, I.G. Kim, N. Matsui, H. Inoue, M. Matsuoka, *Electrochim. Acta* 40 (1995) 561.
- [9] J.-H. Jung, B.H. Liu, J.-Y. Lee, *J. Alloys Comp.* 264 (1998) 306.
- [10] D. Sun, M. Latroche, A. Percheron-Guégan, *J. Alloys Comp.* 248 (1997) 215.
- [11] X. Wang, S. Suda, S. Wakao, *Z. Phys. Chem.* 183 (1994) 297.
- [12] J. Cao, A study on the properties and surface treatment of Zr-based Laves phase hydrogen storage alloys, Ph.D. Thesis, 2000, p. 73.
- [13] J.A. Dean (Ed.), *Lange's Handbook of Chemistry*, 13th Edition, McGraw-Hill Book Company, New York, 1985, pp. 5–6.